Contribution from the Department of Chemistry,
University of Washington, Seattle, Washington 98195

Evidence for Volatile Compounds in the Fe_2O_3–HCl–H_2O–$FeCl_3$ System

N. W. GREGORY

Received April 26, 1983

A spectrophotometric and mass spectrometric study of vapors generated by heating various mixtures in the Fe_2O_3–HCl–H_2O–$FeCl_3$ system is described. The behavior observed in the temperature range 140–350 °C is explained by assuming that along with Fe_2Cl_6 and $FeCl_3$ the molecule H_2OFeCl_3 is present at significant concentrations in the vapor phase. An estimated molar absorptivity of 5000 M^{-1} cm^{-1} at 360 nm is used with the equilibrium absorbance data to derive a standard enthalpy of formation of −141 kcal mol^{-1} and a standard entropy of 113 cal mol^{-1} deg^{-1} for $H_2OFeCl_3(g)$ at 500 K.

Absorbances of vapors, generated by heating mixtures of iron(III) oxide and hydrogen chloride and by heating partially dehydrated samples of the hexahydrate of iron(III) chloride in the temperature range 140–350 °C, have been measured in the UV–visible range of the spectrum. In addition to the absorbance expected from Fe_2Cl_6 and $FeCl_3$, a substantial contribution from other iron-containing molecules is seen. The extra absorbance varies systematically with the partial pressure of hydrogen chloride and water vapor; this behavior, along with mass spectrometric evidence, can be explained if it is assumed that the molecule H_2OFeCl_3 is present in the vapor phase. Absorbance data and an estimated molar absorptivity have been used to estimate thermodynamic properties for this molecule. Results indicate that in the presence of substantial partial pressures of water vapor and of hydrogen chloride, the hydrate contributes in a major way to the amount of iron in the vapor phase at temperatures in the range 150–200 °C and plays an important role in the vapor transport of iron(III) oxide. A number of earlier studies of the Fe_2O_3–HCl–H_2O–$FeCl_3$ equilibrium system have been reported.[1]

Experimental Section

Absorbances were measured with a Cary 14H spectrophotometer. Quartz absorbance cells were cylindrical, ca. 20-mm o.d., with a Pyrex side arm, 5–10 cm long, attached through a graded seal at the center of the cell. Four mixtures of Fe_2O_3 (Baker Analyzed Reagent) and HCl were prepared. HCl, taken from a commercial cylinder (Matheson), was condensed in a liquid nitrogen cooled trap and, after evacuation, vaporized at dry ice temperature into a Pyrex storage bulb. The sample was isolated and this treatment repeated several times. A weighed sample of Fe_2O_3 was introduced into the tip of the cell side arm, the assembly evacuated, and the HCl frozen in by cooling the tip with liquid nitrogen. The quantity of HCl was calculated from a prior measurement of its pressure in a known volume, assuming the perfect gas law. The mixture was then isolated by vacuum flame seal-off of the connecting tube. Identifying sample number, moles of Fe_2O_3, moles of HCl, cell path length (cm), and volume (cm^3), respectively, for the various samples were as follows: 1, 1.44×10^{-4}, 1.73×10^{-4}, 1, 4.41; 2, 6.26×10^{-4}, 4.86×10^{-4}, 5, 15.6; 3, 6.25×10^{-4}, 3.98×10^{-4}, 10, 31.4; 4, 1.88×10^{-4}, 1.99×10^{-4}, 10, 30.9. If the HCl were to react completely with the Fe_2O_3 to form $FeCl_3(H_2O)_{1.5}$, the mole fraction excess of Fe_2O_3 remaining in these mixtures would be the following: 1, 0.67; 2, 0.77; 3, 0.81; and 4, 0.71.

Three other mixtures were prepared by transfer of weighed samples of $FeCl_3(H_2O)_6$ (Baker Analyzed Reagent) into the cell side-arm tips. To reduce the amount of water present, necessary if the vapor absorbance is to be in the measurable range, the cells were evacuated to 10^{-2} torr (10^{-3} for sample 7), and pumping was continued for 30 min. At the onset of pumping the yellow solid changed to reddish color and partially liquefied at room temperature (ca. 22 °C). The samples were then isolated in the absorbance cells by vacuum seal-off of the connecting Pyrex side arm. The folowing are sample identification number, moles of $FeCl_3(H_2O)_6$ initially introduced, cell path length (cm), volume (cm^3), and composition after partial decomposition as calculated from the absorbance data (see discussion section), respectively: 5, 7.41×10^{-5}, 10, 30.0, $FeCl_3(H_2O)_{2.29} + 0.012Fe_2O_3$; 6, 1.59×10^{-4}, 10, 30.2, $FeCl_3(H_2O)_{2.29} + 0.01\ Fe_2O_3$; 7, 1.24×10^{-4}, 5, 15.0, $FeCl_3(H_2O)_{1.95} + 0.16Fe_2O_3$. Some variation in the composition of the partially decomposed samples is to be expected. When these samples are fully vaporized (decomposed) in the absorbance cells, differences in composition will lead to differences in partial pressures of HCl and H_2O and vapor absorbances, as discussed later. Two other samples of $FeCl_3(H_2O)_6$, in Pyrex capillary tubes, were partially dehydrated in the same way and used for the mass spectrometer study.

Cells were placed in a stainless-steel block, with openings for the light beam, and heated with electric furnaces.[2] The temperature of the side-arm tip, T_3, was controlled independently of the cell body, T_1. For the Fe_2O_3–HCl mixtures the condensed phase remained in the tip. The tip was generally kept below the temperature of the cell body (values listed in Table I) to keep deposits from forming on the windows. Because of the opening for the light beam, the windows were always slightly cooler than the cell body. Samples 5, 6, and 7 were controlled similarly in the low-temperature range. However, as shown by the results (see discussion section) at high temperatures, Fe_2O_3 tends to be transported to the high-temperature regions of the cell; hence, under these circumstances T_1 and T_3 were kept closer. Times required for equilibration were long. Mixtures were allowed to stand at randomly selected set temperatures for a minimum of 24 h, often for several days. The absorbance readings were verified by at least two independent approaches to equilibrium.

As described in a previous paper, measurement of the absorbance of iron(III) chloride vapor is complicated by photolytic reduction.[3] Below 250 °C the recombination of $FeCl_2$ and chlorine is slow compared to the rate of photolysis, and continuous exposure to the light beam causes the absorbance of Fe_2Cl_6 in an all-vapor sample to fall at a noticeable rate. To minimize error from this reaction, absorbances were first measured at a set wavelength, 360 nm, the sample being exposed to the light beam for only the few seconds needed to ensure that the instrument had stabilized. The absorbance was then scanned at 1 nm s^{-1} over the range 380–320 nm to observe the shape of the spectrum and to locate the peak maximum in this region. The absorbance at 360 nm was then measured again. A decrease from the initial reading was observed when appreciable amounts of Fe_2Cl_6 were in the vapor phase and a condensed hydrate phase was not present.

Results and Discussion

For each of the mixtures vapor-phase absorbances at 360 nm are listed in Table I and are shown in Figure 1a. The absorption spectrum in each case has a maximum in the vicinity of 360 nm. The temperature dependence of the absorbance at 360 nm of iron(III) chloride vapor (peak maximum 360–365 nm) in equilibrium with $Fe_2O_3(s)$ and FeOCl(s), as reported in an earlier study,[4] is shown as the solid line. Absorbances observed for samples 1–4 lie above this line and in each case appear to approach the line asymptotically as the temperature is increased. It was observed that as the deviation of the absorbance from the line became larger, the wavelength of the absorption peak maximum in the vicinity

(1) See, for example: Schafer, H.; and co-workers. *Z. Anorg. Allg. Chem.* **1949**, *259*, 53, 75, 265; **1949**, *260*, 127; **1950**, *261*, 142; **1952**, *270*, 304.

(2) For experimental setup, see: Hilden, D. L. Ph.D. Thesis, University of Washington, 1971.

(3) Rustad, D. S.; Gregory, N. W. *Inorg. Nucl. Chem. Lett.* **1980**, *16*, 521.

(4) Gregory, N. W. *Inorg. Chem.* **1983**, *22*, 2677.

0020-1669/83/1322-3750$01.50/0

Table I. Absorbance Data

sample	T_1, K	T_3, K	A_{360}	A_x	λ_{max}, nm	sample	T_1, K	T_3, K	A_{360}	A_x	λ_{max}, nm
Range in Which FeOCl(s) and Fe_2O_3(s) Assumed Only Condensed Phases Present											
1	577.2	560.0	1.50[a]		358	3	546.7	514.7	0.152[a]		358
1	560.7	547.0	1.010	0.277	356	3	529.7	513.2	0.147[a]		358
1	540.2	532.7	0.620	0.253	354	3	526.4	501.2	0.0855[a]		358
1	534.7	522.0	0.445	0.237	350	3	494.2	481.2	0.0420	0.0225	350
1	522.4	513.4	0.360	0.228	348	3	493.4	472.0	0.0335	0.0230	348
1	509.0	500.0	0.275	0.212	346	3	497.7	462.7	0.0270	0.0216	352
1	519.0	501.2	0.280	0.215	350	3	477.0	448.4	0.0205	0.0185	348
2	549.0	523.4	0.355	0.137	352	4	523.0	504.2	0.0860[a]		360
2	549.7	522.1	0.345	0.142	350	4	522.0	493.7	0.0525[a]		360
2	527.6	512.4	0.265	0.142	350	4	506.0	490.7	0.0405[a]		360
2	515.4	494.2	0.173	0.130	347	4	506.4	484.4	0.0315	0.0082	360
2	547.7	526.0	0.387	0.135	354	4	490.0	475.2	0.0200	0.0068	357
2	526.4	518.2	0.305	0.133	350	4	484.4	465.7	0.0135	0.0066	356
2	512.7	503.4	0.219	0.144	350	4	470.7	458.2	0.0100	0.0058	355
						4	486.4	471.2	0.0170	0.0069	357
Range in Which Fe_2O_3(s) Assumed Only Condensed Phase Present											
5	458.0	438.0	0.0075	0.0071	338	7	516.4	516.7	0.136	0.084	340
5	474.4	451.2	0.0065	0.0061	340	7	535.7	518.7	0.119	0.0627	342
5	496.4	467.8	0.0063	0.0058	338	7	540.2	530.0	0.118	0.0607	344
6	504.7	480.0	0.0415	0.0369	342	7	564.0	559.0	0.120	0.0567	342
6	507.4	495.4	0.0405	0.0358	342	7	582.8	577.0	0.111	0.0423	342
6	511.0	509.0	0.0373	0.0326	340	7	588.7	576.4	0.106	0.0355	342
6	550.0	530.2	0.0290	0.0232	342	7	599.4	590.7	0.111	0.0369	342
6	552.0	534.4	0.0300	0.0242	340	7	620.7	613.0	0.126	0.0436	342
						7	640.7	632.4	0.134	0.0418	338
Range in Which a Condensed Hydrate Phase Assumed Present											
1	507.2	496.7	0.240	0.223	346	5	442.0	422.0	0.0072	0.0071	338
1	499.4	489.0	0.197	0.156	346	5	437.2	416.4	0.0055	0.0055	335
1	490.4	481.7	0.147	0.124	344	5	430.2	411.4	0.0040	0.0040	335
1	479.7	472.4	0.110	0.100	348	5	436.4	411.4	0.0042	0.0042	335
1	470.0	456.0	0.055	0.0537	350	5	429.7	408.0	0.0032	0.0032	335
2	493.4	476.0	0.117	0.0951	346	6	473.0	413.0	0.0067	0.0067	330
2	481.0	456.0	0.051	0.0489	347	6	474.0	422.4	0.0080	0.0080	330
2	480.4	465.0	0.073	0.0667	344	6	462.0	427.7	0.0150	0.0149	336
2	498.4	479.4	0.127	0.100	346	6	473.2	432.0	0.0145	0.0144	336
2	486.4	472.4	0.105	0.0883	345	6	474.0	436.0	0.0210	0.0208	338
2	474.4	443.0	0.027	0.0267	348	6	473.0	442.0	0.0250	0.0246	338
2	487.7	471.2	0.089	0.0778	345	6	505.2	452.0	0.0430	0.0414	342
2	446.7	442.0	0.025	0.0247	346	6	504.7	455.0	0.0450	0.0430	342
5	447.0	427.2	0.0095	0.0092	340	7	449.0	441.2	0.0220	0.0217	338
5	446.4	426.4	0.0087	0.0085	340	7	465.2	449.7	0.0440	0.0420	340
5	437.4	425.2	0.0082	0.0080	338	7	477.7	458.4	0.0600	0.0548	340
5	441.2	424.4	0.0075	0.0074	338						

[a] Denotes observation shown in Figure 1 but not included in least-squares calculations (see text for explanation).

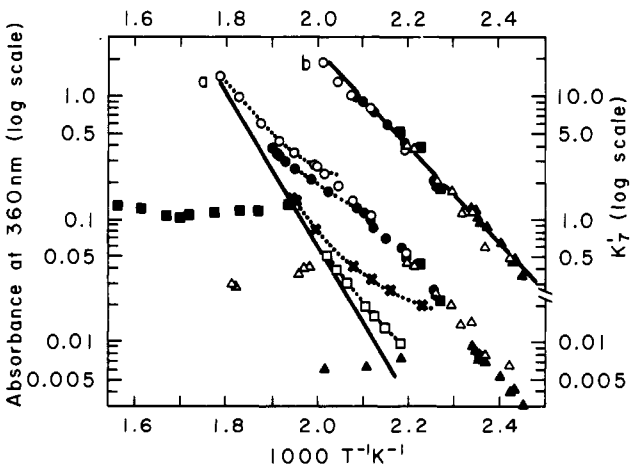

Figure 1. (a) Vapor-phase absorbances at various temperatures ($T = T_3$, except $T = T_1$ for samples 5, 6, and 7 in high-temperature range). Line drawn represents absorbances expected from equilibrium 1. (b) K_7' (see discussion) vs. $1/T_3$. Sample numbers and identifying symbols: 1, ○; 2, ●; 3, ×; 4, □; 5, ▲; 6, △; 7, ■.

of 360 nm became shorter; the smallest values observed were between 330 and 340 nm (Table I). Except for samples 3 and 4, the temperature dependence of the absorbance at lower temperatures changes to an exponential relationship, which suggests that the concentration of the principal absorbing species in that range is controlled by equilibration with a newly formed condensed phase; this phase will be discussed later.

For samples 1–4 at higher temperatures, the following three reactions, of which only two are independent, were initially considered.

$$6FeOCl(s) = 2Fe_2O_3(s) + Fe_2Cl_6(g) \quad (1)$$

$$Fe_2O_3(s) + 6HCl(g) = Fe_2Cl_6(g) + 3H_2O(g) \quad (2)$$

$$Fe_2O_3(s) + 2HCl(g) = 2FeOCl(s) + H_2O(g) \quad (3)$$

If equilibrium 1 fixes the concentration of $Fe_2Cl_6(g)$, and by dissociation $FeCl_3(g)$, the behavior seen in Figure 1a shows that at least one additional molecular species contributes to the absorbance in a major way. It is also apparent that the concentration of this species depends on the amount of hydrogen chloride in the sample. The relationship of the "extra absorbance" to the partial pressure of hydrogen chloride was examined on the following basis. Partial pressures of $Fe_2Cl_6(g)$ were assumed to be given by the values of the equilibrium constant for reaction 1, K_1.[4] Equilibrium constants for reaction 2, K_2, were calculated from recently derived thermodynamic

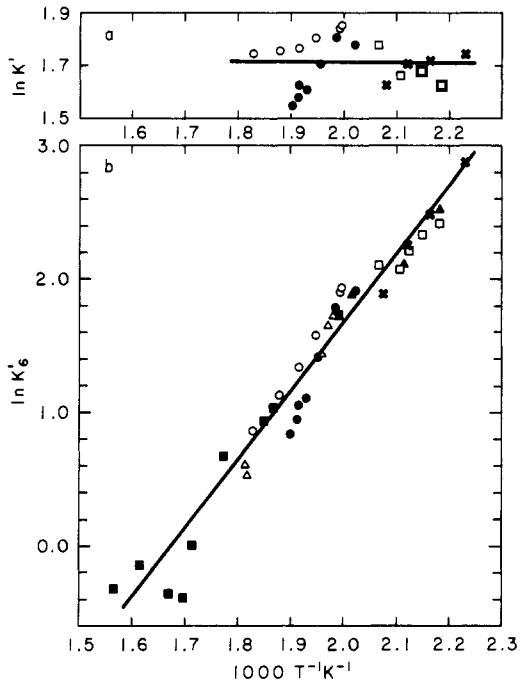

Figure 2. Values derived for K' and K_6' (see discussion) at various temperatures in comparison with least-squares lines (identifying symbols as defined in caption for Figure 1): (a) ln K' vs. $1/T_3$; (b) ln K_6' vs. $1/T$ ($T = T_3$, except $T = T_1$ for samples 5, 6, and 7 in high-temperature range).

constants for $Fe_2Cl_6(g)$[5] and constants for $Fe_2O_3(s)$, HCl(g), and $H_2O(g)$ given in the JANAF tables.[6] In the vicinity of 500 K, these give $\Delta G_2^\circ = -RT \ln K_2 = 323 + 26.41T$ cal mol^{-1}. Values of K_3 may then be derived from the relationship $\Delta G_3^\circ = (\Delta G_2^\circ - \Delta G_1^\circ)/3$, which gives $-RT \ln K_3 = -9990 + 23.50T$ cal mol^{-1}.[4,7] In the range 408–540 K calculated values of K_3 are between 1.7 and 0.07. Thus, in these mixtures reaction 3 is expected to generate substantial amounts of water vapor and FeOCl(s). The absorbances indicate that the concentrations of iron-containing molecules in the vapor phase are small compared to that of water, generally less than 1% (maximum 2%). Hence, in the upper temperature range where Fe_2O_3 and FeOCl are assumed the only condensed phases present, P_{HCl} and P_{H_2O} may be calculated from the equations $n_{HCl}^* RT_1/V = P_{HCl} + 2P_{H_2O} = P_{HCl} + 2K_3P_{HCl}^2$, where n_{HCl}^* is the number of moles of HCl introduced into a cell of volume V, R is the gas constant, and T_1 is the vapor temperature.

The "extra" absorbance at 360 nm, A_x, was calculated as $A - ((E_DP_D + E_MP_M)/RT_1)$, which, in the presence of FeOCl(s) and $Fe_2O_3(s)$, may be written $A - ((E_DK_1 + E_M(K_1/K_D)^{1/2})/RT_1)$. In these expressions A is the total absorbance divided by the cell path length, $E_D = 14011 - 7T_1$, $E_M = 5800$ M^{-1} cm^{-1}, the molar absorptivities[8] of the dimer, Fe_2Cl_6, and monomer, $FeCl_3$, respectively, and P_D and P_M are the corresponding monomer and dimer partial pressures. K_D is the equilibrium constant for the reaction $2FeCl_3(g) = Fe_2Cl_6(g)$, and values at various temperatures were derived from data in the JANAF tables.[6] For the Fe_2O_3–HCl mixtures values of P_M/P_D between 470 and 540 K are small, 0.01–0.05.

For samples 1–4 in the higher temperature range the ratio $A_xRT_1/P_{HCl}^2 = K'$ is found, within the experimental uncertainty, to be constant (see Figure 2a). From the forms of reactions 4 and 5, this behavior would be expected, for example, if either $H_2OFeCl_3(g)$ or $Fe_2(OH)_2Cl_4(g)$, or both, were responsible for the extra absorbance. The P_{HCl} values in the various samples differ substantially, a factor of 5 larger in sample 1 than in sample 4. Mass spectrometric data, discussed later, give evidence for the presence of H_2OFeCl_3 in vapors emitted from freely vaporizing condensed hydrate samples, and, as shown below, the behavior of samples 5–7 can also be explained if H_2OFeCl_3 is assumed primarily responsible for the extra absorbance. With this assumption K' would correspond to K_4E_x, where E_x is the molar absorptivity (unknown) of the hydrate vapor molecule.

$$FeOCl(s) + 2HCl(g) = H_2OFeCl_3(g) \quad (4)$$

$$2FeOCl(s) + 2HCl(g) = Fe_2(OH)_2Cl_4(g) \quad (5)$$

Values of A marked with an asterisk in Table I were not included in Figure 2a because the uncertainty in the measurement has an increasingly larger effect on A_x as the total absorbance approaches the line for reaction 1, that is, as the contribution of Fe_2Cl_6 becomes dominant. A least-squares treatment of the 22 values included in Figure 2a gives the equation $\ln K' = -18.8T_3^{-1} + 1.752$; the standard deviation of ln K' is 5.1% As reflected by the very small enthalpy constant, the variation of K' with temperature falls within the scatter of the points.

It will be seen in Figure 1a that the behavior of samples 5–7 at higher temperatures is quite different from that of samples 1–4. Absorbances are below those predicted for reaction 1 and, over most of the range, decrease as the temperature is increased. This behavior is expected if partial pressures of water vapor are too high to permit formation of the FeOCl(s) phase. Since the amounts of water and chloride left in these samples were not known, these quantities were fixed by calculation so as to give the best fit of the absorbance data when it is assumed that reaction 2, the monomer–dimer equilibrium, and reaction 6 determine the equilibrium state. K_6' corresponds to $K_3K_2'^2$ and values at various temperatures may be calculated from equations given above. Again, concentrations of iron-containing molecules in the vapor phase are very small compared to those expected for HCl and H_2O if the reaction $FeCl_3(H_2O)_{1.5+x} = 0.5Fe_2O_3(s) + 3HCl(g) + xH_2O(g)$ is assumed to be complete in the high-temperature range. The number of moles of HCl and H_2O may then be treated as constants; their values for each sample were determined by a least-squares fit of an equation based on the relationship

$$Fe_2O_3(s) + 6HCl(g) = 2H_2OFeCl_3(g) + H_2O(g) \quad (6)$$

$$ART_1 = E_xP_x + E_DP_D + E_MP_M = (K'(K_3)^{1/2}G^5)n_{H_2O}X + (E_DK_2G^6)X^2 + (E_M(K_2/K_D)^{1/2}G^3)X$$

where $G = (RT/V)^{1/2}$ and $X = (n_{HCl}/(n_{H_2O})^{1/2})^3$. The derived mole numbers are shown as the corresponding starting compositions listed in the Experimental Section.

To show the overall correlation, values of P_{HCl} and P_{H_2O} were calculated from the derived number of moles and, with K_2 and K_D, the contributions of Fe_2Cl_6 and $FeCl_3$ to the absorbance evaluated and subtracted from the total. The resulting values of $K_6' = (A_xRT_1)^2P_{H_2O}/P_{HCl}^6$, together with corresponding values for samples 1–4, are shown in Figure 5b. A combined least-squares treatment of the 39 observations gave the equation $\ln K_6' = 5155T^{-1} - 8.640$. The standard deviation of the enthalpy constant was 3.9% and of the entropy constant 4.5%. The predicted ratios P_{H_2O}/P_{HCl}^2 for samples 5–7 in the high-temperature range are larger than K_3, as required if the FeOCl(s) phase is not formed.

When $Fe_2O_3(s)$ is the only condensed phase present and amounts of HCl and H_2O in the vapor are virtually constant, the concentration of H_2OFeCl_3 appears to decrease as the temperature increases. An increase in the total absorbance at the highest temperatures, as seen for sample 7, may be

(5) Rustad, D. S.; Gregory, N. W. *J. Chem. Eng. Data* **1983**, *28*, 151.
(6) "JANAF Thermochemical Tables" (Supplements); Dow Chemical Co.: Midland, MI, Sept 30, 1964 (HCl), June 30, 1965 (Fe_2O_3, $FeCl_3$, Fe_2Cl_6), and March 31, 1979 (H_2O).
(7) See also: Stuve, J. M.; Ferrante, M. J.; Richardson, D. W.; Brown, R. R. *Rep. Invest.—U.S., Bur. Mines* **1980**, *RI-8420*.
(8) Schafer, H.; Binnewies, M.; Florke, U. *Z. Anorg. Allg. Chem.* **1981**, *477*, 31.

explained by an increased contribution from $FeCl_3(g)$. With samples 5–7 the approach to equilibrium was particularly slow at temperatures just above the temperature at which the condensed hydrate phase disappears; no values are shown in this range on Figure 1a. One expects, from the temperature dependence of K_6', that $H_2OFeCl_3(g)$ will serve as a means of transporting Fe_2O_3 from T_3 to T_1. It appears that this process is slow and that the temperature of the condensed phase in the intermediate range is not well-defined. After the measurements at high temperatures, a film of what appeared to be Fe_2O_3 was seen in the T_1 regions of the sample 5–7 cells. For the least-squares calculations, and in Figure 2b, T_1 was taken as the temperature that fixes the equilibrium concentrations for these samples. For samples 1–4 amounts of Fe_2O_3 introduced were substantially larger and FeOCl(s) was formed. The bulk of these solids remained in the tip at T_3, which was taken as the equilibrium-controlling temperature.

Except for samples 3 and 4 the absorbances at lower temperatures appear to be controlled by the presence of a condensed hydrate phase. If $Fe_2O_3(s)$ and FeOCl(s) are also present, the composition of all phases will be fixed at a given temperature, regardless of the starting composition. While absorbances for samples 1 and 2 do appear to lie on a common line, an extrapolation of this line to the range for samples 5 and 6 does not agree well with the observed values. The correlation is noticeably improved if it is assumed that the condensed hydrate phase is $FeCl_3(H_2O)_{0.5}$ and that FeOCl(s) is not present. In such a case the partial pressure of H_2OFeCl_3 would depend on the partial pressure of water, as shown by reaction 7. The relative amounts of HCl and H_2O in the lower

$$FeCl_3(H_2O)_{0.5}(liq) + 0.5H_2O(g) = H_2OFeCl_3(g) \quad (7)$$

temperature range would then be fixed by the condensation reaction (8) and the relationship $P_{H_2O} = P_{H_2O}^* + (P_{HCl}^* - P_{HCl})/3$, where the P^* values represent pressures expected from the total numbers of moles of H_2O and HCl, respectively, derived above for the high-temperature limit (samples 5–7) or known from the method of preparation (samples 1 and 2). By substitution of $P_{H_2O} = K_6'P_{HCl}^6/(A_xRT_1)^2$, the resulting sixth-power equation was solved for P_{HCl}. A_x was initially taken as $ART_1 - E_DP_D - E_MP_M$ with P_D and P_M fixed by equilibrium 1. The derived values of P_{HCl} and P_{H_2O} were then used with K_2 and K_D to recalculate P_D and P_M, and the calculation was repeated (three iterations gave consistent results). Data from the five samples were used to derive values of $K_7' = A_xRT_1/P_{H_2O}^{1/2}$, which are shown in Figure 1b. The line drawn represents the least-squares solution for the 33 observations, $\ln K_7' = -8960T_3^{-1} + 21.05$. Standard deviations of the constants were 1.9% and 1.8%, respectively, small considering the uncertainty of the measurements. However, it seems not unlikely that the composition of the condensed hydrate phase may vary with temperature and the composition of the vapor, and its nature cannot be clearly established by these limited observations.[12]

$$0.5Fe_2O_3(s) + 3HCl(g) = FeCl_3(H_2O)_{0.5}(liq) + H_2O(g) \quad (8)$$

When absorbances were measured with a condensed hydrate phase present, effects of a photolysis reaction were readily apparent. Unexpectedly, instead of a decrease in absorbance, observed when Fe_2O_3 and FeOCl were the only condensed phases present (see Experimental Section), continuous exposure to the light beam was accompanied by an increase in the total absorbance. With sample 1 at 210 °C, for example, an exposure of ca. 30 min was accompanied by an increase of the absorbance from the value shown on Figure 1a to a value corresponding roughly to an extrpolation of the sample 1 dotted line drawn through the points in the higher temperature range. When the light was shut off and the absorbance measured only intermittently, the value decreased back to the equilibrium value shown on Figure 1a. The following explanation in terms of the proposed reactions seems plausible but has not been proven.

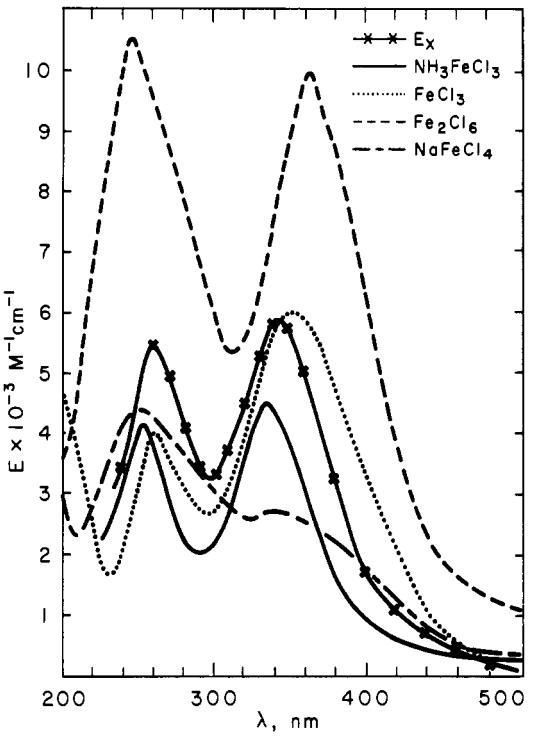

Figure 3. Molar absorptivity vs. wavelength for various iron(III) vapor molecules (vicinity of 300 °C). E_x values at various wavelengths were calculated from the "extra absorbance" by using the concentration given by the estimated value E_x = 5000 M^{-1} cm^{-1} at 360 nm.

The photolytic reaction appears to be mainly the reduction of $Fe_2Cl_6(g)$.[3] When the absorbing vapor was predominately H_2OFeCl_3, e.g., samples 5–7 at higher temperatures, no change in concentration (no photolysis) was noticed during the period of a scan from 600 to 250 nm (5–6 min). If Fe_2O_3 and $FeCl_3(H_2O)_x$ are the only condensed phases present for sample 1 at 210 °C, concentrations of the vapor species may be assumed fixed by equilibrium reactions like (2), (7), and (8); alternatively, (2) and (8) may be combined to give a reaction like (9). As the concentration of Fe_2Cl_6 is reduced by photolysis, the concentrations of water vapor (reaction 9 to the right), HCl (reaction 8 to the left), and H_2OFeCl_3 (reaction 7 to the right) may be expected to increase. If the increase in absorbance from the increased concentration of H_2OFeCl_3 more than offsets the reduced contribution from the loss of Fe_2Cl_6, the total absorbance will increase. The observed behavior suggests that continued photolysis leads to the disappearance of the condensed hydrate phase and a P_{H_2O}/P_{HCl}^2 ratio such that FeOCl is formed, by reactions 3 or 4, and the absorbance returns to values expected for equilibrium 4. In the dark the original equilibrium mixture is regenerated. A further study of this system is planned.

$$2FeCl_3(H_2O)_{2x}(liq) = Fe_2Cl_6(g) + 2xH_2O(g) \quad (9)$$

Mass Spectrometric Studies. The capillary tubes containing samples of partially dehydrated $FeCl_3(H_2O)_6$ were placed, in separate experiments, in the direct-insertion probe of a Hewlett-Packard 5985 GC mass spectrometer. The end of the capillary tube was cut off at the moment of insertion, and ion masses generated from vapor molecules leaving the condensed phase in the high vacuum of the source chamber were observed in the range 50–350 amu. During the first few minutes, with the source temperature ca. 110 °C, significant contributions at mass numbers 109, 111 (H_2OFeCl^+) and 144, 146

($H_2OFeCl_2^+$) and 179, 181, 183 ($H_2OFeCl_3^+$), along with ions expected from $FeCl_3$ and Fe_2Cl_6, were observed. At about 1 min mass peak 91 ($FeCl^+$) had the maximum intensity and the 109 peak a relative intensity of 19%. Around 2 min the 254 peak ($Fe_2Cl_4^+$) had maximum intensity, with 109 at 40%. After about 3 min the hydrate peaks had essentially merged into the background, to be expected after water vapor and hydrogen chloride have been removed by the vacuum system. Ions from the iron(III) chloride molecules persisted somewhat longer. The second sample duplicated the behavior observed with the first. Ions that could be identified exclusively as formed by parent molecules, such as $Fe_2(OH)_2Cl_4$ or related hydroxy halide dimers, were not above background level. While such molecules might, nevertheless, be important in the equilibrium systems, their presence does not seem to be required to explain the absorbance and mass spectrometric behavior observed in the present study. Mass spectrometric evidence for the presence of traces of oxy and hydroxy chlorides of aluminum in aluminum chloride vapor in contact with quartz or glass[8] and traces of hydroxy chlorides of iron in iron(III) chloride vapor containing small amounts of water as an impurity[9] has recently been reported.

A_x Absorption Spectrum in the Range 250–600 nm. The absence of appreciable photolytic effects and the position of the absorption peak maximum around 340 nm for vapors of samples 5–7 indicate that Fe_2Cl_6 and $FeCl_3$ contribute to the total absorbance in only a minor way. A_x values at various wavelengths from data from sample 7 at 280 °C were converted to estimated molar absorptivities by using a concentration based on the estimated value $E_x = 5000$ M^{-1} cm^{-1} at 360 nm, comparable to values for $FeCl_3$[10] and NH_3FeCl_3.[11] The resulting spectrum is shown in Figure 3 in comparison with spectra of other iron(III) chloride vapor molecules. The A_x spectrum is very similar to that reported for NH_3FeCl_3[11] and is believed to be associated with charge-transfer transitions. The bonding and structure of H_2OFeCl_3 and H_3NFeCl_3 would be expected to be similar, with the iron atom bonded to three chlorine atoms and an oxygen (or nitrogen) atom in an approximately tetrahedral configuration. The concentration estimated indicates that the iron in the vapor of this sample is largely in the form of the hydrate molecule; the derived ratio $P_x/(P_x + P_D + P_M)$, where P_x is the partial pressure of H_2O-$FeCl_3$, is 0.9. For the mixtures included in Figure 1a this ratio varies from 0.4 to nearly unity and shows a general correlation with the shift in the wavelength of the absorption peak maximum. Ratios will be smaller if E_x is actually larger than the assumed value.

Estimated Thermodynamic Properties. The estimated molar absorptivity, temperature dependence neglected, together with the equilibrium constant expressions derived above give, for reaction 4, $\Delta G_4° = 37 + 13.44T$ cal mol^{-1} and, for reaction 6, $\Delta G_6° = -10244 + 51.02T$ cal mol^{-1}. Together with thermodynamic constants for the other substances in reactions 4 and 6 taken from references cited above, the constants in these free energy equations give −141 kcal mol^{-1} for the standard enthalpy of formation and 113 cal mol^{-1} deg^{-1} for the standard entropy of $H_2OFeCl_3(g)$ at 500 K. These values seem reasonable although data for similar hydrate vapor molecules have not been found for comparison. The derived entropy is, of course, sensitive to the uncertainty of the value estimated for E_x. The result projects, for example, for the dissociation reaction $H_2OFeCl_3(g) = FeCl_3(g) + H_2O(g)$, $\Delta G° = 22000 - 29.0T$ cal mol^{-1}, which may be compared with $\Delta G° = 34550 - 34.0T$ cal mol^{-1} for $Fe_2Cl_6(g) = 2FeCl_3(g)$. In the latter case dissociation requires the rupture of two Fe–Cl bridge bonds as compared with a single Fe–O bond in the former, assuming the proposed structure.

Registry No. Fe_2O_3, 1309-37-1; $FeCl_3$, 7705-08-0; H_2OFeCl_3, 60684-13-1; HCl, 7647-01-0.

(9) Naumova, T. N.; Zhevnina, L. S.; Poponova, R. V.; Chupakhjin, M. S.; Stepin, B. D. *Russ. J. Inorg. Chem.* (*Engl. Transl.*) **1979**, *24*, 10.
(10) Rustad, D. S.; Gregory, N. W. *Inorg. Chem.* **1977**, *16*, 3036.
(11) Gregory, N. W. *Inorg. Chem.* **1981**, *20*, 3667.
(12) Results of a subsequent study (with D. S. Rustad) of mixtures with much lower partial pressures of water correlate better with present data when the condensed hydrate phase is assumed to be $FeCl_3(H_2O)$. This indicates tht the improved correlation noted in this paragraph, using $FeCl_3(H_2O)_{0.5}$, may not be significant relative to overall experimental error.

Contribution from the Departments of Chemistry, Wayne State University, Detroit, Michigan 48202, and Illinois Institute of Technology, Chicago, Illinois 60616

Electron-Transfer Reactivity in Some Simple Cobalt(III)–Cobalt(II) Couples. Franck–Condon vs. Electronic Contributions[1]

JOHN F. ENDICOTT,*† GEORGE R. BRUBAKER,*†‡ T. RAMASAMI,† KRISHAN KUMAR,† KADDI DWARAKANATH,† JONATHAN CASSEL,† and DAVID JOHNSON‡

Received August 9, 1982

Electron-transfer rates involving the $Co(sep)^{3+,2+}$ (sep = 1,3,6,8,10,13,16,19-octaazabicyclo[6.6.6]eicosane) and $Co(en)_3^{3+,2+}$ couples have been examined for any differences in contributions of Franck–Condon and electronic terms to the rate constants. Rate constants for cross-reaction oxidations of $Co(sep)^{2+}$ follow the classically predicted dependence of the Franck–Condon factor on $\Delta G_{ab}°$. Far-infrared and Raman vibrational spectra of $M(sep)^{3+}/M(en)_3^{3+}$ (M = Co, Rh) are in very close correspondence. As a consequence, the force constants of the M–N stretching modes must also be comparable (differing by less than 10%) in the $Co(sep)^{3+}$ and $Co(en)_3^{3+}$ complexes. Strain energy calculations based on these and other published force constants are consistent with the differences in self-exchange rates and indicate upper limits on the Franck–Condon term in the rate constants consistent with significant contributions from electronic factors in both exchange reactions.

Introduction

A current concern in the study of electron-transfer reactivity relates to the significance of donor–acceptor electronic interactions in determining reactivity.[2-17] Thus, the bimolecular rate constant may be formulated[2-6,8]

$$k = K_o\nu^2[G(FC)]$$

† Wayne State University.
‡ Illinois Institute of Technology.

(1) Partial support of this research by the National Institutes of Health (Grant No. AM 14341) and by the Department of Energy (Grant No. ER-78-S-02-4685) is gratefully acknowledged.

0020-1669/83/1322-3754$01.50/0